

# Liquid Structure of the Ionic Liquid 1,3-Dimethylimidazolium Bis{(trifluoromethyl)sulfonyl}amide

Maggel Deetlefs,<sup>†</sup> Christopher Hardacre,<sup>\*,†</sup> Mark Nieuwenhuyzen,<sup>†</sup> Agilio A. H. Padua,<sup>‡</sup> Oonagh Sheppard,<sup>†</sup> and Alan K. Soper<sup>§</sup>

School of Chemistry and Chemical Engineering, The QUILL Centre, Queen's University Belfast, Belfast BT9 5AG, United Kingdom, Laboratoire de Thermodynamique des Solutions et des Polymères, Université Blaise Pascal/CNRS, Clermont-Ferrand, France, and Rutherford Appleton Laboratory, Chilton, Didcot, Oxon, OX11 0QX, United Kingdom

Received: February 13, 2006; In Final Form: April 20, 2006

Neutron diffraction has been used to determine the liquid structure of 1,3-dimethylimidazolium bis{(trifluoromethyl)sulfonyl}amide ([dmim][NTf<sub>2</sub>]). Significantly smaller charge ordering is found in this liquid compared with analogous chloride and hexafluorophosphate salts due to the diffuse charge density and size of the [NTf<sub>2</sub>]<sup>−</sup> anion. This is manifested in a much larger cation–cation and cation–anion separation and an overlap of the cation–cation and cation–anion shells. Comparison of the liquid structure with the crystal structure reported by Holbrey et al. (*Dalton Trans.* 2004, 2267) indicates little correlation, for example, the [NTf<sub>2</sub>]<sup>−</sup> anion adopts a trans orientation predominantly in the liquid whereas a cis orientation is found in the solid phase.

## Introduction

Over the past decade the importance of room temperature ionic liquids has grown significantly. Interest in this class of solvent stems from the properties exhibited by the liquids (including effectively zero vapor pressure) and the ease by which many of these properties may be varied. Many of these materials are based around the imidazolium cation 1-alkyl-3-methylimidazolium ([C<sub>n</sub>mim]<sup>+</sup>) shown in Figure 1. Simply by changing the anion, for example, [BF<sub>4</sub>]<sup>−</sup>, [PF<sub>6</sub>]<sup>−</sup>, [CF<sub>3</sub>CO<sub>2</sub>]<sup>−</sup>, or [(CF<sub>3</sub>SO<sub>2</sub>)<sub>2</sub>N]<sup>−</sup>, or the alkyl chain on the cation, a wide range of tunable properties can be obtained, for example, hydrophobicity, viscosity, and density. This area has been the subject of an increasing number of publications and reviews.<sup>1</sup> In general, most of the research performed to date on ionic liquids has concentrated on electrochemical processes and their use as a reaction medium, although increasingly many other applications have been described, for example, their use as lubricants<sup>2</sup> and sensors<sup>3</sup> and in analytical chemistry.<sup>4</sup> However, data on the liquid structure of these liquids are limited.

There have been a number of theoretical studies examining the structure and properties of ionic liquid systems using, for example, molecular dynamics,<sup>5</sup> molecular force fields,<sup>6</sup> ab initio,<sup>7</sup> and Monte Carlo approaches.<sup>8</sup> In contrast, experimental data are less readily available. Neutron diffraction has been employed to investigate the structure of 1,3-dimethylimidazolium ([dmim]<sup>+</sup>) chloride and hexafluorophosphate ionic liquids.<sup>9,10</sup> In each case, comparison of the diffraction of deuterated and protiated liquids enabled a detailed picture of the anion–cation and cation–cation interactions to be described. Strong charge ordering was observed with similar anion–cation interactions for both anions. In both cases, there was a strong

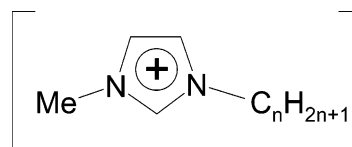


**Figure 1.** 1-Alkyl-3-methylimidazolium [C<sub>n</sub>mim]<sup>+</sup> structure, when *n* = 1 the structure represents the [dmim]<sup>+</sup> cation studied in this paper.

correlation between the solid-state structure and the liquid structure. Neutron and X-ray reflectivity has also been used to investigate the structure of both long and short alkyl chain length imidazolium based ionic liquids.<sup>11</sup> The ionic liquids were found to be layered with the ionic and alkyl parts of the liquid segregating into a lamellar structure. This ordering is maintained to at least two alkyl chain lengths. However, the uncertainty in the analysis did not allow a determination of whether the charged layer is at the surface or how deep the ordering penetrates in the liquid.

The structure of binary ionic liquids has been examined by both neutron and X-ray diffraction. Takahashi et al. studied the structures of AlCl<sub>3</sub>:[C<sub>2</sub>mim]Cl mixtures over a range of concentrations from 46 to 67 mol % of AlCl<sub>3</sub>.<sup>12</sup> Above 50 mol % of AlCl<sub>3</sub>, the [Al<sub>2</sub>Cl<sub>7</sub>]<sup>−</sup> anion geometry was found to change in the liquid compared with the isolated ions implying a direct interaction between the imidazolium cation and the anionic species. Mixtures of HCl and [C<sub>2</sub>mim]Cl have also been studied.<sup>13,14</sup> By analyzing the first order differences using hydrogen/deuterium substitution on both the imidazolium ring and the HCl, two intramolecular peaks were observed. These indicated the presence of [HCl<sub>2</sub>]<sup>−</sup> as an asymmetric species. More recently, high-energy X-ray diffraction has been used to examine the liquid structure of binary ionic liquids of 1,3-dialkylimidazolium fluoride with HF.<sup>15</sup> As found for 1,3-dimethylimidazolium salts studied by neutron diffraction, the X-ray data showed that the solid state and liquid structures are closely related showing the presence of [HF<sub>2</sub>]<sup>−</sup> in both phases. Shodai et al. also studied the structure of liquid [(CH<sub>3</sub>)<sub>4</sub>N]<sup>+</sup>F<sup>−</sup>.

\* Address correspondence to this author. Phone: +44-28-9097-4592. Fax: +44-28-9097-4687. E-mail: c.hardacre@qub.ac.uk.

<sup>†</sup> Queen's University Belfast.

<sup>‡</sup> Université Blaise Pascal/CNRS.

<sup>§</sup> Rutherford Appleton Laboratory.

$n\text{HF}$  ( $n = 3-5$ ). A range of anion structures were found in the liquid,  $[(\text{HF})_x\text{F}]^-$  ( $x = 1-3$ ); however, structures with higher ratios of HF to  $\text{F}^-$  ( $x = 4$  or  $5$ ) were not found in the melt although similar compositions have been reported in the solid state.<sup>16</sup>

As well as the pure ionic liquids, the liquid structure of solutions of ionic liquids with solutes has been determined by using neutron and X-ray diffraction and IR and NMR correlated with theoretical studies. For example, Deetlefs et al. showed on dissolution of benzene in  $[\text{dmim}][\text{PF}_6]$  that, while strong charge ordering in the ionic liquid remained, the cation–cation distribution is changed significantly.<sup>17</sup> The cations are also found to interact predominantly with the ring of the benzene while the anions interact with the ring hydrogens to a first approximation. As with the pure ionic liquids, similar interactions are also found in the solid.<sup>18</sup> This is supported by analogous molecular dynamics simulations.<sup>19</sup> The solvation of carbon dioxide<sup>20</sup> and water<sup>21</sup> has also been examined with vibrational spectroscopy and in each case the solute was found to interact mainly with the anion and not the cation. As found with benzene, the experimental data and theory show good agreement.<sup>22</sup>

An understanding of the structure of the ionic liquid and dissolved substances is important if the reactivity and selectivity found in ionic liquid mediated reactions is to become predictive. For example, through the understanding of water–ionic liquid reactions, the remarkable hydrolytic stability of phosphorus trichloride and oxychloride when solubilized in wet bis- $\{(\text{trifluoromethyl})\text{sulfonyl}\}\text{amide}$  and perfluorophosphate-containing ILs, respectively, may be understood.<sup>23</sup> This is thought to be due to a strong hydrogen bonding interaction between the water and the anion, which breaks up the water–water interactions and decreases the nucleophilicity of the water thus reducing its hydrolysis activity.

This paper reports the liquid structure of 1,3-dimethylimidazolium bis- $\{(\text{trifluoromethanesulfonyl})\}\text{amide}$  with use of neutron diffraction. Bis- $\{(\text{trifluoromethanesulfonyl})\}\text{amide}$  based ionic liquids are among the most commonly used ionic liquids due to their hydrophobicity, high thermal stability, and relatively low viscosity.<sup>24</sup> The liquid structure obtained is compared with a molecular force field simulation and a recently reported X-ray crystal structure of  $[\text{dmim}][\text{NTf}_2]$ .<sup>25</sup>

## Experimental Section

1,3-Dimethylimidazolium bis- $\{(\text{trifluoromethyl})\text{sulfonyl}\}\text{-amide}$  ( $[\text{dmim}][\text{NTf}_2]$ ) were synthesized from the appropriate deuterated and protiated 1,3-dimethylimidazolium chloride<sup>26</sup> salts by metathesis with  $\text{LiNTf}_2$ .<sup>24</sup> For salts with a deuterated cation ring, the metathesis was performed in deuterium oxide to prevent ring H–D exchange. The samples were analyzed by  $^1\text{H}$  and  $^2\text{H}$  NMR, IR, and elemental analysis showing  $>97\%$  isotopic exchange in each case. All samples were dried as liquids under high vacuum at 353 K, cooled, and stored under  $\text{N}_2$  prior to being loaded into the sample cells.

The samples were heated to 303 K in aluminum sample holders with 0.2 mm thick vanadium windows were sealed by using a PTFE coated Viton “o” ring while in the diffraction vacuum chamber and left for 10 min to equilibrate before measurements were taken. The temperature was maintained to  $\pm 0.1^\circ$  by using a Eurotherm PID temperature controller. Measurements were made on each of the empty sample holders, the empty spectrometer, and a 3.1 mm thick vanadium standard sample for the purposes of instrument calibration and data normalization. After appropriate normalization for the cell and the window type, good reproducibility was found between the

**TABLE 1: Lennard-Jones and Coulomb Parameters Used for the Reference Potential of the Simulation of the 1,3-Dimethylimidazolium Cation ( $[\text{dmim}]^+$ )**

atom	$\sigma/\text{\AA}$	$\epsilon/\text{kJ mol}^{-1}$	$q_{\text{cation}}^{\text{A}}/e$	$q_{\text{cation}}^{\text{B}}/e$
H(2)	1.6	0.05000	0.097	0.210
C(2)	3.9	0.79396	0.407	−0.110
H(4,5)	1.6	0.05000	0.094	0.210
C(4,5)	3.9	0.79396	0.105	−0.130
N(1,3)	3.4	0.57341	−0.267	0.300
C(M)	3.9	0.79396	0.124	−0.170
H(M)	1.6	0.05000	0.064	0.130

**TABLE 2: Lennard-Jones and Coulomb Parameters Used for the Reference Potential of the Simulation of the Bis- $\{(\text{trifluoromethyl})\text{sulfonyl}\}\text{amide}$  Anion ( $[\text{NTf}_2]^-$ )**

atom	$\sigma/\text{\AA}$	$\epsilon/\text{kJ mol}^{-1}$	$q_{\text{anion}}^{\text{A}}/e$	$q_{\text{anion}}^{\text{B}}/e$
N	3.4	0.57341	−0.267	−0.660
S	2.0	0.70000	0.348	1.020
O	3.0	0.45000	−0.075	−0.530
C	3.9	0.79396	0.407	0.350
F	3.0	0.59560	−0.290	−0.160

sample cells. The neutron diffraction data were taken with the SANDALS diffractometer at the ISIS pulsed neutron source, Rutherford Appleton Laboratory, U.K. This instrument has a wavelength range of 0.05 to 4.5  $\text{\AA}$  and data are taken over the  $Q$  range of 0.05 to 50  $\text{\AA}^{-1}$ .

The data were analyzed with the standard ATLAS package<sup>27</sup> to produce a differential scattering cross section for each sample. Four samples with different hydrogen isotope substitutions—namely fully protiated, fully deuterated, a 1:1 fully deuterated: fully protiated mixture, and side chain deuterated only—were measured. These different samples served to highlight the structure around different parts of the molecule. In addition by using the difference in the neutron scattering cross sections for  $^1\text{H}$  and  $^2\text{H}$  this provides a number of datasets which could be compared with the simulation thus increasing the confidence in the derived structure. The liquid sample had a density of 0.085 atoms  $\text{\AA}^{-3}$ .<sup>28</sup> The neutron diffraction data were fitted by using the empirical potential structure refinement process (EPSR).<sup>29</sup> The full parameters of the reference potential used as input parameters for the EPSR process are given in Tables 1 and 2 for the cation and anion, respectively. Two sets of charges were compared for both the cation and anion to understand the sensitivity of the structure obtained to the charges used. Cation charges ( $q_{\text{cation}}^{\text{A}}$ ) were derived by Hanke et al.<sup>5</sup> and the anion charges ( $q_{\text{anion}}^{\text{A}}$ ) were calculated as Löwdin charges from an optimized anion structure at the 6-31++G\*/B3LYP level of theory in GAMMES. The comparative cation and anion charges used ( $q_{\text{cation}}^{\text{B}}$ ,  $q_{\text{anion}}^{\text{B}}$ ) were derived by Lopes and Padua.<sup>30</sup> The carbon and nitrogen atoms are defined as their position on the *molecular* skeleton with M referring to the methyl groups. The hydrogen atoms, H( $x$ ), are defined as being bonded to the  $x$  carbon atom. The Lennard-Jones parameters for interactions between unlike atoms were calculated by employing the usual Lorentz–Berthelot mixing rules.

## Results and Discussion

Figure 2 shows a comparison of the experimental neutron diffraction (symbols) and the fit derived from the EPSR model (lines) by using the potential derived from  $q_{\text{cation/anion}}^{\text{A}}$  atomic charges for 1,3-dimethylimidazolium bis- $\{(\text{trifluoromethanesulfonyl})\}\text{amide}$  as a function of  $Q$ . The plots show that there is good agreement between the derived structure factors of each sample and the experimental data. Similarly good agreement is found for all other combinations of charges used.

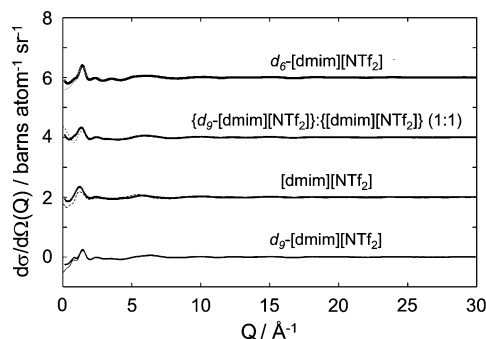


**Figure 2.** Experimental (symbols) and EPSR fitted (line) differential cross sections as a function of  $Q$  for the 1,3-dimethylimidazolium bis-((trifluoromethyl)sulfonyl)amide at 303 K.

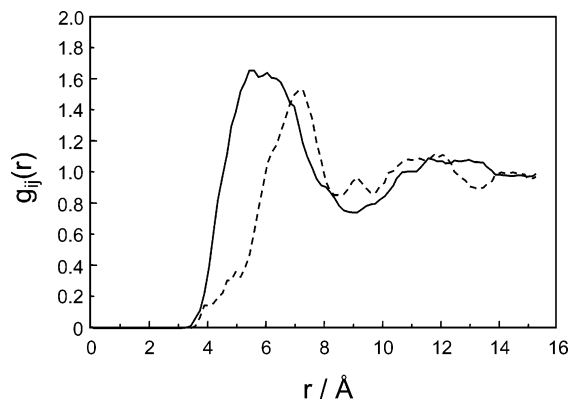


**Figure 3.** Comparison of the partial radial distribution functions for the cation–anion distribution (solid line) and the cation–cation distribution (dashed line) for [dmim][NTf<sub>2</sub>] at 303 K derived from the EPSR model by using the cation and anion atomic charges  $q^{\text{A}_{\text{cation}}}$  and  $q^{\text{A}_{\text{anion}}}$ , respectively. Each radial distribution function is calculated from the center of the imidazolium ring and from the nitrogen atom of the [NTf<sub>2</sub>]<sup>−</sup> anion.

From the EPSR model using  $q^{\text{A}_{\text{cation/anion}}}$  atomic charges the cation–anion and cation–cation partial radial distributions around a central imidazolium cation are shown in Figure 3. The cation–cation (center–center) contact distance is centered at  $\sim 7.0$  Å with the cation–anion (center–center) distance slightly shorter centered at  $\sim 5.2$  Å. A comparison of the cation–cation contacts for the 1,3-dimethylimidazolium bis-((trifluoromethyl)sulfonyl)amide with the chloride<sup>9</sup> (5.5 Å) and hexafluorophosphate<sup>10</sup> (6.3 Å) salts shows that the cation-to-cation contacts become larger as the size of the anion is increased,  $\text{Cl}^- < [\text{PF}_6]^- < [\text{NTf}_2]^-$ . A similar trend is also seen for the cation–anion interactions with the chloride<sup>9</sup> ( $\sim 4.2$  Å) and hexafluorophosphate<sup>10</sup> ( $\sim 4.5$  Å) salts. This is indicative of an expansion of the liquid structure as compared to [dmim]Cl and [dmim][PF<sub>6</sub>]. Although the anion shell is at a shorter distance from the central cation compared with the cation shells, as expected from a charge ordered system and as seen in the analogous chloride and hexafluorophosphate salts, it is clear that the long-range alternating structure of cations and anions found in the Cl<sup>−</sup> and [PF<sub>6</sub>]<sup>−</sup> based salts does not exist in [dmim][NTf<sub>2</sub>]. This is obvious in the second shells for the cations and anions in [dmim][NTf<sub>2</sub>] at  $\sim 13$  Å where the anion and cation peaks are almost coincident.

The probability distributions of the cation and anion around a central imidazolium cation are shown in Figure 4. At high probabilities, shown in Figure 4a, the anion shows a clear preference for positions associated with the face of the ring system. Moreover, even at lower probabilities (Figure 4b) little anion density is observed axial to the ring hydrogens. This is

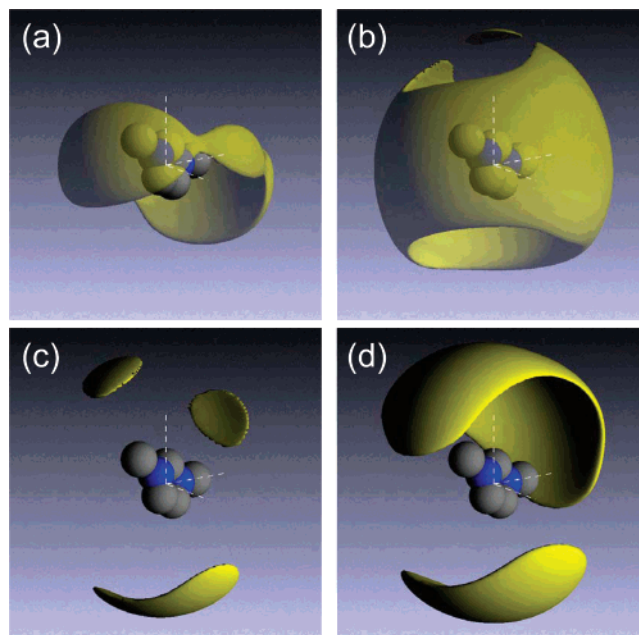


**Figure 4.** Probability distributions of (a, b) the bis-((trifluoromethyl)sulfonyl)amide anion and (c, d) the imidazolium cation around an imidazolium cation derived from the EPSR model for [dmim][NTf<sub>2</sub>] at 303 K, using the cation and anion atomic charges  $q^{\text{A}_{\text{cation}}}$  and  $q^{\text{A}_{\text{anion}}}$ , respectively. For distributions a and c the contour level was chosen to enclose the top 5% of the molecules while for distributions b and d the contours enclose the top 20% of molecules each in the distance range 0–9 Å.

in complete contrast with the anion spatial probability distribution observed in the case of [dmim]Cl, for example, where the hydrogen bonding to the C(2) hydrogen, in particular, and the C(4,5) hydrogens is strong. Although some anion density is also located above and below the imidazolium ring in [dmim]Cl at high probabilities, it is only at low probabilities that this becomes pronounced. An intermediate spatial anion distribution was observed for the analogous [PF<sub>6</sub>]<sup>−</sup> system, namely that the anion density axial to the ring decreases  $\text{Cl}^- > [\text{PF}_6]^- > [\text{NTf}_2]^-$  whereas the opposite is true for the facial anion density  $\text{Cl}^- < [\text{PF}_6]^- < [\text{NTf}_2]^-$ . This may be understood by the increasingly diffuse nature of the negative charge and increasing size of the anion comparing chloride, hexafluorophosphate, and bis-((trifluoromethyl)sulfonyl)amide. As the ions increase in size and the charge becomes more delocalized, the hydrogen bonding ability of the anion decreases thus reducing the bonding strength with the acidic ring protons. In the chloride salt, the hydrogen bonding dominates the spatial distribution, whereas with reduced hydrogen bonding ability, the electrostatic interactions and steric factors become more important and the anion becomes more likely to be associated with the ring system. The more diffuse charge density on the anion also results in softer Coulombic interactions between the cation and anion and hence the reduction in charge ordering observed in the partial radial distribution functions. When using a cutoff corresponding to the first minimum in the cation–anion partial radial distribution function, i.e., 6.4 ([dmim]Cl), 7.5 ([dmim][PF<sub>6</sub>]), and 9.0 Å ([dmim][NTf<sub>2</sub>]), there are 6, 6.8, and 8.8 anions in the first shell, respectively. The large increase in the anion population in the first shell of the [NTf<sub>2</sub>]<sup>−</sup> salt is due to the larger cation–anion separation as a result of the decreased charge ordering and Coulombic interactions.

A comparison of the anion spatial density map with that of the cation surrounding a central cation (panels a and b in Figure 4 compared with panels c and d) shows that the cations and



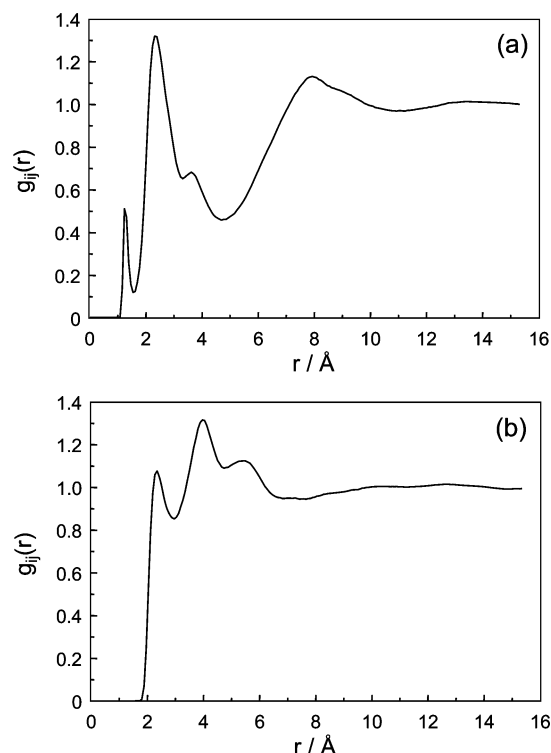


**Figure 5.** Partial radial distribution functions of (a) the methyl hydrogen–methyl hydrogen and (b) the methyl hydrogen–fluorine found in the EPSR model of [dmim][NTf<sub>2</sub>], using the cation and anion atomic charges  $q^{\text{A}}_{\text{cation}}$  and  $q^{\text{A}}_{\text{anion}}$ , respectively.

anions occupy mutually exclusive positions, even when 20% of the ions are considered. Even at low probability no cation density is found above or below the imidazolium ring, which is in contrast with the anion spatial density where the majority of ions interact with the cation  $\pi$  system. A similar mutually exclusive arrangement of anions and cations was also observed in the [dmim][PF<sub>6</sub>] liquid structure; however, this is more pronounced in the liquid structure of [dmim][NTf<sub>2</sub>]. In [dmim][PF<sub>6</sub>], the size of the anion coupled with the drive to high ion density was proposed as the cause of this packing arrangement. Replacing the [PF<sub>6</sub>]<sup>−</sup> with a much larger [NTf<sub>2</sub>]<sup>−</sup> anion will exacerbate the need for the cations and anions to be in different areas of the spatial distribution.

To examine the structure in more detail the partial radial distribution functions of the methyl hydrogen–fluorine (cation–anion) and methyl hydrogen–methyl hydrogen (cation–cation) are shown in Figure 5. At first glance it would be easy to infer from the methyl hydrogen–fluorine partial radial distribution function that there was some sort of hydrogen bonding interaction between these hydrogen atoms and the fluorine atoms. This interpretation fails to take into account the size and shape of the bis{(trifluoromethyl)sulfonyl}amide anion. The bis{(trifluoromethyl)sulfonyl}amide anions are associated with the centers of the imidazolium rings and the distribution extends along the cation N–N vector toward the methyl groups (Figure 4b). Thus this association is due to the size of the anions. No significant hydrogen bonding is observed in the system due to the diffuse nature of the negative charge on the anion. Comparison of the methyl–methyl distance with the methyl fluorine distance both centered at  $\sim 3.0$  Å reinforces the observation that these interactions are due to ion packing rather than hydrogen bond formation (Figure 5). In fact CF<sub>3</sub>⋯H hydrogen bonds have been shown to be at best very weak by van den Berg et al.<sup>31</sup> Furthermore, <sup>19</sup>F–<sup>1</sup>H NOE NMR measurements by Mele et al. have shown that there are no

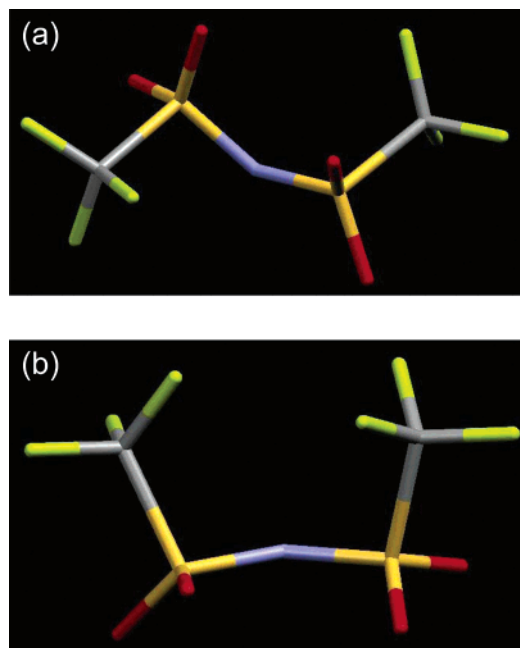


**Figure 6.** Models showing (a) the trans and (b) the cis configuration of the bis{(trifluoromethyl)sulfonyl}amide anion.<sup>25</sup>

interactions between the CF<sub>3</sub> moieties of the anions and the hydrogen atoms of the cations.<sup>32</sup>

From the EPSR model, the ratio of the cis/trans orientation of the [NTf<sub>2</sub>]<sup>−</sup> group (Figure 6) may be obtained. Figure 7a shows the number of anions as a function of the intramolecular CF<sub>3</sub>⋯CF<sub>3</sub> distance. There is clearly a bimodal distribution of distances with maxima at a CF<sub>3</sub>⋯CF<sub>3</sub> distance of  $\sim 4.2$  and  $\sim 5.2$  Å corresponding to the cis and trans forms, respectively, and  $\sim 80\%$  of the anions exist in the trans state. Recently, molecular force field simulations have also been performed to examine the liquid structure of [C<sub>n</sub>mim][NTf<sub>2</sub>].<sup>30</sup> From this simulation, a similar distribution of CF<sub>3</sub>⋯CF<sub>3</sub> distances was found in [dmim][NTf<sub>2</sub>], as shown in Figure 7a. Clearly a strong correlation of the two distributions is observed despite the change in methodology used in each case.<sup>33</sup> From the models, the torsion angle of the C–S⋯S–C bond may be calculated and shows maxima at  $\sim 40^\circ$  and  $170^\circ$  for the cis and trans arrangements, respectively, as shown in Figure 7b from the molecular force field simulations.

For many of the ionic liquid simulations performed to date, a range of atomic charges have been used on the cation and anion. To examine the effect of changing the atomic charges on the liquid structure, a series of EPSR simulations were performed with use of the charges shown in Tables 1 and 2. Figure 8 shows a comparison of the radial distribution functions with a range of cation and anion atomic charges ( $q^{\text{A}}_{\text{cation}}$ ,  $q^{\text{B}}_{\text{cation}}$ ,  $q^{\text{A}}_{\text{anion}}$ ,  $q^{\text{B}}_{\text{anion}}$ ). On changing the cation atomic charges from  $q^{\text{A}}_{\text{cation}}$  to  $q^{\text{B}}_{\text{cation}}$  with a common set of anion atomic charges similar anion–cation and cation–cation radial distributions were found. By increasing the atomic charges on the anion from  $q^{\text{A}}_{\text{anion}}$  to  $q^{\text{B}}_{\text{anion}}$ , although the cation–anion radial distribution remains similar with the anion feature centered at  $\sim 6.0$  Å, the cation–cation radial distribution shifts such that the nearest neighbors are centered at  $\sim 8.0$  Å ( $q^{\text{B}}_{\text{anion}}$ ) compared with  $\sim 7.5$  Å ( $q^{\text{A}}_{\text{anion}}$ ).

The small effect on the radial distribution of the atomic charges on the cation skeleton is expected as the interactions between ions will be dominated by the outer atoms, i.e., the hydrogen atoms, and similar charges have been used for both simulations. In contrast the outer atoms on the anions have much

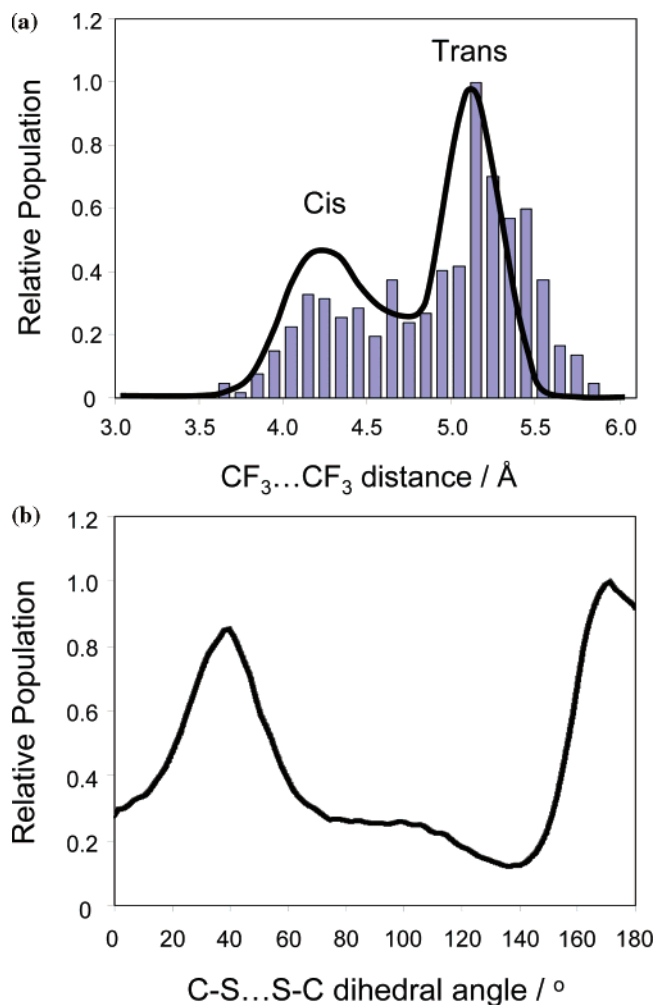


**Figure 7.** Distribution of the (a)  $\text{CF}_3\cdots\text{CF}_3$  distances and (b)  $\text{C-S}\cdots\text{S-C}$  dihedral angle as a function of the number of anions in liquid [dmim][NTf<sub>2</sub>]. In panel a the distribution derived from the EPSR model with use of the  $q^{\text{A}_{\text{cation}}}$  and  $q^{\text{A}_{\text{anion}}}$  atomic charges is shown as bars. In panels a and b the molecular force field method developed by Lopes and Padua<sup>30</sup> is shown as a solid line.

larger charges derived from the molecular force field approach than calculated from the Löwdin simulation. This leads to an increased ion separation in the radial distribution function and consequently more charge ordering, as expected. However, despite the difference in charges in both cases, the charge ordering is still substantially less than that found in [dmim][PF<sub>6</sub>] or [dmim]Cl due to the delocalization of the charge over the anion. This has a major influence on the properties of the [NTf<sub>2</sub>]<sup>−</sup> based ionic liquids. For example, the viscosity of these liquids are, in general, much lower than those found for the corresponding [PF<sub>6</sub>]<sup>−</sup> and Cl<sup>−</sup> salts due to the much softer ionic structure, which allows the ions to move more freely with respect to one another. In addition, the weaker Coulombic interactions reduce the ability of the long -chain [NTf<sub>2</sub>]<sup>−</sup> based ionic liquids to form liquid crystals<sup>34</sup> as the charged layer becomes more diffuse and the anion can encroach into the aliphatic region weakening the structural motif that defines the liquid crystal structure.

It is useful to make a comparison of the available chloride, hexafluorophosphate, and bis{(trifluoromethyl)sulfonyl}amide 1,3-dimethylimidazolium crystal structures to examine whether the trends within the solids are also characteristic of the melts.

In the solid-state structure of [dmim]Cl, hydrogen-anion contacts dominate the interionic interactions.<sup>35</sup> Each chloride

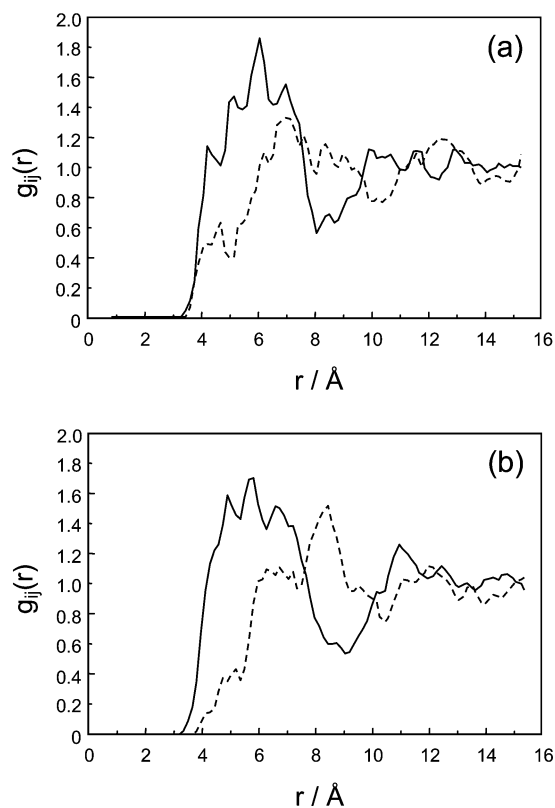


**Figure 8.** Comparison of the partial radial distribution functions for the cation-anion distribution (solid line) and the cation-cation distribution (dashed line) for the [dmim][NTf<sub>2</sub>] at 303 K derived from the EPSR model by using the cation and anion atomic charges (a)  $q^{\text{B}_{\text{cation}}}$  and  $q^{\text{A}_{\text{anion}}}$  and (b)  $q^{\text{A}_{\text{cation}}}$  and  $q^{\text{B}_{\text{anion}}}$ . Each radial distribution function is calculated from center of the imidazolium ring and from the nitrogen atom of the [NTf<sub>2</sub>]<sup>−</sup> anion.

is in close contact with seven hydrogen atoms, three chloride-ring hydrogen atom contacts are found between 2.6 and 2.7 Å, and the methyl hydrogen-chloride contacts range from 2.7 to 2.9 Å. These distances are expanded to approximately 4.5 Å in the liquid phase. Each imidazolium is surrounded by 6 anions, in agreement with the liquid structure, with one of the chloride ions interacting with the top of the imidazolium ring as well as with the methyl group from an adjacent cation. From the crystal structure, the cations form dimer motifs held by methyl hydrogen- $\pi$  and  $\pi$ - $\pi$  interactions associated with methyl hydrogen-ring nitrogen and C(4,5)-C(4,5) short contacts, respectively. The closest distance between the cations is found between two methyl hydrogens from imidazolium rings in adjacent dimers at 2.5 Å. Although this is simply a van der Waals contact distance, and therefore not associated with any attractive interaction, it is interesting to note that in the liquid, the anion-cation interactions, which, to a first approximation, control the structure, are sufficiently similar to also make the shortest cation-cation contacts between adjacent methyl hydrogens.

Within the [dmim][PF<sub>6</sub>] crystal structure, the imidazolium cations form a weakly  $\text{C-H}\cdots\pi$  hydrogen bonded zigzag chain motif via CH<sub>3</sub> and the imidazolium ring  $\pi$ -system along the (0 0 1) direction.<sup>18</sup> The [PF<sub>6</sub>]<sup>−</sup> ions are located between these chains and make closest contacts with the methyl hydrogens. Furthermore, because of the zigzag nature of the imidazolium H-bonded chains the [PF<sub>6</sub>]<sup>−</sup> anions are also associated with the  $\pi$ -system of the cations. As found for the 1,3-dimethylimidazolium chloride salt, the solid-state crystal structure and the liquid structure of [dmim][PF<sub>6</sub>] are very similar. For example,

the large “holes” in the cation–cation distribution are found in both the liquid and solid states. Moreover, in both states, short cation–cation contacts are found between methyl hydrogens with little interaction between the H(2) and H(M) positions and the anion predominantly interacts with the ring and not the ring hydrogens. Overall the structures of 1,3-dimethylimidazolium chloride and hexafluorophosphate are very similar despite the difference in hydrogen bonding ability. However, due to the size of the hexafluorophosphate anion compared with the chloride, the structure is expanded. Unlike for the chloride salt, the spatial distributions of the anions and cations in the hexafluorophosphate salt have an almost mutually exclusive arrangement.

The structure of 1,3-dimethylimidazolium bis{(trifluoromethyl)sulfonyl}amide<sup>25</sup> shows the cations to be aligned in layers within the lattice. The cationic layers are able to interact with one another giving  $\pi\cdots\pi$  (C–C) interactions at 3.55 Å. However, the shortest contact between cations is still the H(M)–H(M) van der Waals contact of 3.05 Å, which is also an interlayer contact. The liquid structure of [dmim][NTf<sub>2</sub>] shows no evidence of any  $\pi\cdots\pi$  interactions. The reason for this is a consequence of the inherent flexibility of the [NTf<sub>2</sub>]<sup>−</sup> anion. From an examination of bis{(trifluoromethyl)sulfonyl}amide based structures in the Cambridge crystallographic database the majority of anions (~95%) are found in the trans conformation as found in the liquid structure reported herein. However, this does not correlate well with the crystal structure of [dmim][NTf<sub>2</sub>]. Therein a cis arrangement of the [NTf<sub>2</sub>]<sup>−</sup> anion was observed, as shown in Figure 6b. Therefore, unlike for the [dmim][PF<sub>6</sub>] and [dmim]Cl liquid structures, where a strong correlation of the liquid structure was found with the crystal structure, for [dmim][NTf<sub>2</sub>] this is not found to be the case. It would seem reasonable to suppose that this uncommon conformation has consequences for the cations within this structure and that this material probably exists as conformational polymorphs although only one has been characterized to date. Therefore, it is not possible to draw any conclusions about the liquid structure based on the characterized solid unlike in many of the other systems examined.

Polymorphism is not uncommon in ionic liquid crystals and has been examined in detail in a number of cases. For example, crystal polymorphism has been reported for 1-alkyl-3-methylimidazolium tetrachloropalladate(II) salts ([C<sub>n</sub>mim]<sub>2</sub>[PdCl<sub>4</sub>], *n* = 10–18)<sup>36</sup> where up to three separate crystal phases were noted. Similarly, two alkyl chain conformations have been observed for short and long alkyl chain halide based methylimidazolium salts. Thermal treatment of the salts allows the alkyl chain to relax and transform between gauche-gauche and trans-gauche conformations<sup>37</sup> as well as bent and linear ring–alkyl chain arrangements.<sup>38</sup>

## Conclusion

The liquid structures of the 1,3-dimethylimidazolium chloride, hexafluorophosphate, and bis(trifluoromethanesulfonyl)amide salts show a decreasing affinity for hydrogen bonding with the cation as a function of both charge density and anion size. Unlike the chloride and hexafluorophosphate salts, the solid state structure of the bis(trifluoromethanesulfonyl)amide salt shows little similarity with the liquid structure. This is due probably to the conformational flexibility of the anion, which is found in the trans conformation mainly in the liquid state compared with the cis conformation reported for the solid state. The trend for the anion to be associated with the  $\pi$  system of the ring is found to increase with the size of the anion and the decrease in

the charge density, i.e., Cl<sup>−</sup> < [PF<sub>6</sub>]<sup>−</sup> < [NTf<sub>2</sub>]<sup>−</sup>, with the opposite trend found for the anion density associated with the ring hydrogens.

**Acknowledgment.** O.S. acknowledges support from the Department of Education and Learning in Northern Ireland and Merck GmbH. M.D. thanks QUILL, the Royal Society, and EPSRC for funding. CCLRC are thanked for the allocation of the beamtime. C.H. and AP thanks the Royal Society and CentACat for funding. Dr. J. A. van den Berg is thanked for help with calculating the anion charges.

## References and Notes

- (1) *Ionic Liquids in Synthesis*; Wasserscheid, P.; Welton T., Eds.; Wiley-VCH Verlag: Weinheim, Germany, 2003.
- (2) Ye, C. F.; Liu, W. M.; Chen, Y. X.; Yu, L. G. *Chem. Commun.* **2001**, 2244.
- (3) Yu, L.; Garcia, D.; Rex, R. B.; Zeng, X. Q. *Chem. Commun.* **2005**, 2277.
- (4) Berthod, A.; Carda-Broch, S. *Actual. Chim.* **2004**, 271, 24.
- (5) For example: Hanke, C. G.; Price, S. L.; Lynden-Bell, R. M. *Mol. Phys.* **2001**, 99, 801.
- (6) For example: Lopes, J. N. C.; Deschamps, J.; Padua, A. A. H. *J. Phys. Chem. B* **2004**, 108, 2038.
- (7) For example: Del Popolo M. G.; Lynden-Bell, R. M.; Kohanoff, J. *J. Phys. Chem. B* **2005**, 109, 5895.
- (8) For example: Shah, J. K.; Maginn, E. J. *Fluid Phase Equilibria* **2004**, 222, 195. Shah, J. K.; Maginn, E. J. *J. Phys. Chem. B* **2005**, 109, 10395.
- (9) Hardacre, C.; Holbrey, J. D.; McMath, S. E. J.; Bowron, D. T.; Soper, A. K. *J. Chem. Phys.* **2003**, 118, 273.
- (10) Hardacre, C.; McMath, S. E. J.; Nieuwenhuyzen, M.; Bowron, D. T.; Soper, A. K. *J. Phys. C* **2003**, 15, S159.
- (11) Bowers, J.; Vergara-Gutierrez, M. C.; Webster, J. R. P. *Langmuir* **2004**, 20, 309. Solutskin, E.; Ocko, B. M.; Taman, L.; Kuzmenko, I.; Gog, T.; Deutsch, M. J. *Am. Chem. Soc.* **2005**, 127, 7796. Carmichael, A. J.; Hardacre, C.; Holbrey, J. D.; Nieuwenhuyzen, M.; Seddon, K. R. *Mol. Phys.* **2001**, 99, 795.
- (12) Takahashi, S.; Suzuya, K.; Kohara, S.; Koura, N.; Curtiss, L. A.; Saboungi, M.-L. *Z. Phys. Chem.* **1999**, 209, 209.
- (13) Truelove, P. C.; Haworth, D.; Carlin, R. T.; Soper, A. K.; Ellison, A. J. G.; Price, D. L. *Proceedings of the 9th International Symposium on Molten Salts*, San Francisco Electrochemistry Society: Pennington, NJ, 1994; Vol. 3, p 50.
- (14) Trouw, F. R.; Price, D. L. *Annu. Rev. Phys. Chem.* **1999**, 50, 571.
- (15) Hagiwara, R.; Matsumoto, K.; Tsuda, T.; Ito, Y.; Kohara, S.; Suzuya, K.; Matsumoto, H.; Miyazaki, Y. *J. Non-Cryst. Solids* **2002**, 312–314, 414. Matsumoto, K.; Hagiwara, R.; Ito, Y.; Kohara, S.; Suzuya, K. *Nucl. Instrum. Methods Phys. Res. B* **2003**, 199, 29.
- (16) Shodai, Y.; Kohara, S.; Ohishi, Y.; Inaba, M.; Tasaka, A. *J. Phys. Chem. A* **2004**, 108, 1127.
- (17) Deetlefs, M.; Hardacre, C.; Nieuwenhuyzen, M.; Sheppard, O.; Soper, A. K. *J. Phys. Chem. B* **2005**, 109, 1593.
- (18) Holbrey, J. D.; Reichert, W. M.; Nieuwenhuyzen, M.; Sheppard, O.; Hardacre, C.; Rogers, R. D. *Chem. Commun.* **2003**, 476.
- (19) Harper, J. B.; Lynden-Bell, R. M. *Mol. Phys.* **2004**, 102, 85. Hanke, C. G.; Johansson, A.; Harper, J. B.; Lynden-Bell, R. M. *Chem. Phys. Lett.* **2003**, 374, 85.
- (20) Kanakubo, M.; Umecky, T.; Hiejima, Y.; Aizawa, T.; Nanjo, H.; Kameda, Y. *J. Phys. Chem. B* **2005**, 109, 13847. Kazarian, S. G.; Sakellarios, N.; Gordon, C. M. J. *Chem. Soc., Chem. Commun.* **2002**, 1314. Kazarian, S. G.; Briscoe, B. J.; Welton, T. *Chem. Commun.* **2000**, 2047.
- (21) Mele, A.; Tran, C. D.; Lacerda, S. H. D. *Angew. Chem., Int. Ed.* **2003**, 42, 4364. Cammarata, L.; Kazarian, S. G.; Salter, P. A.; Welton, T. *Phys. Chem. Chem. Phys.* **2001**, 3, 5192.
- (22) Hanke, C. G.; Lynden-Bell, R. M. *J. Phys. Chem. B* **2003**, 107, 10873. Cadena, C.; Anthony, J. L.; Shah, J. K.; Morrow, T. I.; Brennecke, J. F.; Maginn, E. J. *J. Am. Chem. Soc.* **2004**, 126, 5300.
- (23) Amigues, E.; Hardacre, C.; Keane, G.; Migaud, M.; O'Neill, M. *Chem. Commun.* **2006**, 72.
- (24) Bonhôte, P.; Dias, A. P.; Papageorgiou, N.; Kalyanasundram, K.; Grätzel, M. *Inorg. Chem.* **1996**, 32, 1168.
- (25) Holbrey, J. D.; Reichert, W. M.; Rogers, R. D. *Dalton Trans.* **2004**, 2267.
- (26) Hardacre, C.; Holbrey, J. D.; McMath, S. E. J. *J. Chem. Soc., Chem. Commun.* **2001**, 367.
- (27) Soper, A. K.; Howells, W. S.; Hannon, A. C. *ATLAS—Analysis of Time-of-Flight Diffraction Data from Liquid and Amorphous Samples*; Rutherford Appleton Laboratory, Report RAL-89-046, 1989.

- (28) Fannin, A. A.; Floreani, D. A.; King, L. A.; Landers, J. S.; Piersma, B. J.; Stech, D. J.; Vaughn, R. L.; Wilkes, J. S.; Williams, J. L. *J. Phys. Chem.* **1984**, *88*, 2614.
- (29) Soper, A. K. *Chem. Phys.* **1996**, *202*, 295. Soper, A. K. *Chem. Phys.* **2000**, 258, 121. Soper, A. K., *Mol. Phys.* **2001**, *99*, 1503.
- (30) Lopes, J. N. C.; Padua, A. A. H. *J. Phys. Chem. B* **2004**, *108*, 16893.
- (31) van den Berg, J. A.; Seddon, K. R. *Cryst. Growth Des.* **2003**, *3*, 643.
- (32) Mele, A. Unpublished data.
- (33) To generate the distributions shown in Figure 7 from the molecular force field approach, the molecular dynamics simulations were ran on systems consisting of 200 ion pairs (time step of 1 fs, cutoff of 16 Å, Ewald summations). The initial configuration was a low-density random arrangement that was equilibrated for 500 ps. The production run had a duration of 200 ps from which 1000 snapshots were saved for the calculation of the conformational histograms.
- (34) Bradley, A. E.; Hardacre, C.; Holbrey, J. D.; Johnston, S.; McMath, S. E. J.; Nieuwenhuyzen, M. *Chem. Mater.* **2002**, *14*, 629.
- (35) Arduengo, A. J.; Dias, H. V. R.; Harlow, R. L.; Kline, M. *J. Am. Chem. Soc.* **1992**, *114*, 5530.
- (36) Hardacre, C.; Holbrey, J. D.; McCormac, P. B.; McMath, S. E. J.; Nieuwenhuyzen, M.; Seddon, K. R. *J. Mater. Chem.* **2001**, *11*, 346.
- (37) Hamaguchi, H.; Saha, S.; Ozawa, R.; Hayashi, S. Ionic Liquids IIIA: Fundamentals, Progress, Challenges and Opportunities, Properties and Structure. *ACS Symp. Ser.* **2005**, *901*, 68. Ozawa, R.; Hayashi, S.; Saha, S.; Kobayashi, A.; Hamaguchi, H. *Chem. Lett.* **2003**, *32*, 948.
- (38) Downard, A.; Earle, M. J.; Hardacre, C.; McMath, S. E. J.; Nieuwenhuyzen, M.; Teat, S. J. *Chem. Mater.* **2004**, *16*, 43.